Dual *in vitro* and *in silico* analysis of thiacalix[4]arene dinaphthalene sulfonate for the sensing of 4-nitrotoluene and 2,3-dinitrotoluene

Krunal Modi,[a*] Urvi Panchal[b] , Chirag Patel[c], Keyur Bhatt[d], Shuvankar Dey[b], Divya Mishra[b], V.K.Jain[b]

[a.] *J. Heyrovsky Institute of physical Chemistry, Academy of Sciences of the Czech Republic,* Dolejškova2155/3, 182 23 Prague 8, Czech Republic.
[b.] Department of Chemistry, University School of Sciences, Gujarat University, Ahmedabad , Gujarat, India, 380 009.
[c.] Department of Botany, Bioinformatics and Climate Change Impacts Management, University School of Science, Gujarat University, Ahmedabad-380 009, Gujarat, INDIA..
[d.] Department of Chemistry, Ganpat university, Kherwa, Gujarat, India, 384 012.

Supplementary material

S1 Materials and Methods

Chemicals and reagents

All reagents and solvents were obtained from Spectrochem, Merck or Sigma Aldrich and used without further purification. Thin layer chromatography was carried out on silica gel 60 F_{254} silica-aluminum plates, and the plates were visualized using ultraviolet light. Column chromatography was performed on silica gel 75-150 µm (100-200 mesh) supplied by Spectrochem (India).

Instruments

All the glassware was dried overnight in an oven before use. The mass analysis was performed using the ESI technique on a Q-TOF (micromass) spectrometer. NMR data were recorded on a Bruker AV(III)-400 MHz with a BBFO probe. All samples were analyzed in $CDCl_3$. The reference values for residual solvent were taken as δ=7.27($CDCl_3$) for ^{1}H-NMR and δ=77.1 ($CDCl_3$) for ^{13}C-NMR. The multiplicities for coupled signals were designated using the abbreviations s= singlet, d= doublet, dd= doublet of doublets, ddd= doublet of doublet of doublets, and m= multiplets, and all frequencies are given in hertz. Elemental analysis (C, H, N and S) was performed on vario MICRO-Variant elemental analyzer (Mt.Laurel, USA). A VEEGO (Model No. VMP-DS) melting point apparatus (Mumbai, India) was used to measure the melting points (uncorrected) in a single capillary tube. The fluorescence spectra were recorded using a Jasco FP-8300 spectrofluorometer (Tokyo, Japan) with EHCS-813.

General procedure for detection of NACs by spectrofluorometry:

Using 5% water:THF as the solvent, 2 x 10^{-4} M stock solutions of TCDNS and the various NACs [1,3-DNB (1,3-dinitrobenzene); 2,3-DNT (2,3-dinitrotoluene); 2,4-DNT (2,4-dinitrotoluene); 2,6-DNT (2,6-dinitrotoluene); 4-NT (4-nitrotoluene); MNA (N-methyl-4-nitroaniline); 2-NT(2-nitrotoluene); NB (nitrobenzene); TNT (trinitrotoluene); and TNP (trinitrophenol)] were prepared. In each 5 ml volumetric flask, 2.5 ml of the stock solution of TCDNS and 2.5 ml of the stock solution of one of the NACs were taken, so that the effective concentration of each of TCDNS and the NAC was 1 x 10^{-4} M. The emission studies were performed using the as-prepared solutions. A Job plot study (method of continuous variation) was also performed on this basis.

The same stock solution of TCDNS and the metal ions was used for the emission studies. For each solution, 2.5 ml was mixed in a 5 ml volumetric flask and used for titration. Then, all the spectra for the spectrofluorimetric studies were recorded and compared. The binding constants of TCDNS with the 2,3-DNT and 4-NT complexes were determined by previously reported methods.

Molecular Docking

Molecular docking has become an essential tool in computational modelling. The purpose is to conceive ligands with specific electrostatic and stereochemical attributes to achieve high receptor binding affinity. The availability of three-dimensional macromolecular structures enables a diligent inspection of the binding site topology, including the presence of clefts, cavities and sub-pockets. The electrostatic properties, such as the charge distribution, can also be carefully examined [1, 2].

The chemical structures of TCDNS with 4-NT and 2,3-DNT were developed by the geometry optimization technique from Gaussian G09[3]. The optimized structures were given as the starting host (TCDNS) and guest (4-NT and 2,3-DNT) for the Accelry's Discovery Studio software, version 4.0. The energy scores are calculated based on 3D knowledge based shapes from the superimposed pair of the host and guest forming the host-guest complex. The complex with the best docked score is retrieved by molecular docking with AUTODOCK version 4.2. The complex with the lowest free energy is also identified. The docking energy was calculated by the equation

$$\Delta G = \Delta G_{vdW} + \Delta G_{Hbond} + \Delta_{Gelec} + \Delta G_{tor} + \Delta G_{desolv}$$

where the terms for the docking energy are

ΔG_{vdW} = van der Waals

ΔG_{Hbond} = H bonding

ΔG_{elec} = electrostatic
ΔG_{tor} = torsional free energy term for ligand when the ligand transits from unbounded to bounded state
ΔG_{desolv} = desolvation

Host-guest interactions

To obtain insight into the possible host-guest interactions, particularly the non-covalent interactions that cannot be determined by spectrofluorimetric results, molecular docking studies can be performed. Non-covalent interactions play a major role in depicting the various host-guest interactions that are rendered using the Accelry's Discovery Studio visualizer version 16.1. These include hydrogen bonds, hydrophobic interactions, π-alkyl hydrophobic interactions, π-cationic interactions and π-π interactions.

Molecular dynamics simulation

The geometrically optimized structure allows the observation of several intermolecular features supporting the process of molecular recognition. Structural descriptions of the host-guest complexes are useful for the investigation of the binding conformations, the characterization of key intermolecular interactions, the characterization of unknown binding sites, mechanistic studies and the elucidation of ligand-induced conformational changes[4]. Usually, the ligand stabilizes a subset of several possible conformations of the receptor, shifting the equilibrium toward the minimum energy structures [5].

Molecular dynamics (MD) can be used to estimate the stability of a ligand-receptor complex proposed by molecular docking [6]. Molecular dynamics applies Newton's equations of motion, as described in classical mechanics, to specify the position and speed of each atom in the system under study. As a result, the trajectory and temporal evolution of a host-guest complex can be examined [7]. Initially, a specific configuration is attributed to the atoms with the purpose of reproducing the temperature and pressure of the real system. From the computation of the forces acting on each particle, it is possible to determine the position and velocity of each of these atoms at a later time. These calculations are repeatedly performed until the molecular trajectories are integrated for a given time interval [8]. Schrodinger's Desmond v3.6 was used for the MD simulation studies.

The MD simulation study was performed for a duration of 50 ns with a relaxation time of 1 ps at a constant temperature of 300 K, in addition to a constant volume and shape ensemble (NVT) with a Nose-Hoover thermostat. The structural changes and dynamic behavior of the complex were investigated by estimating the root mean square deviation (RMSD). MD stimulation analysis has been divided into main two parts. (1) Quality analysis; (2) Event analysis.

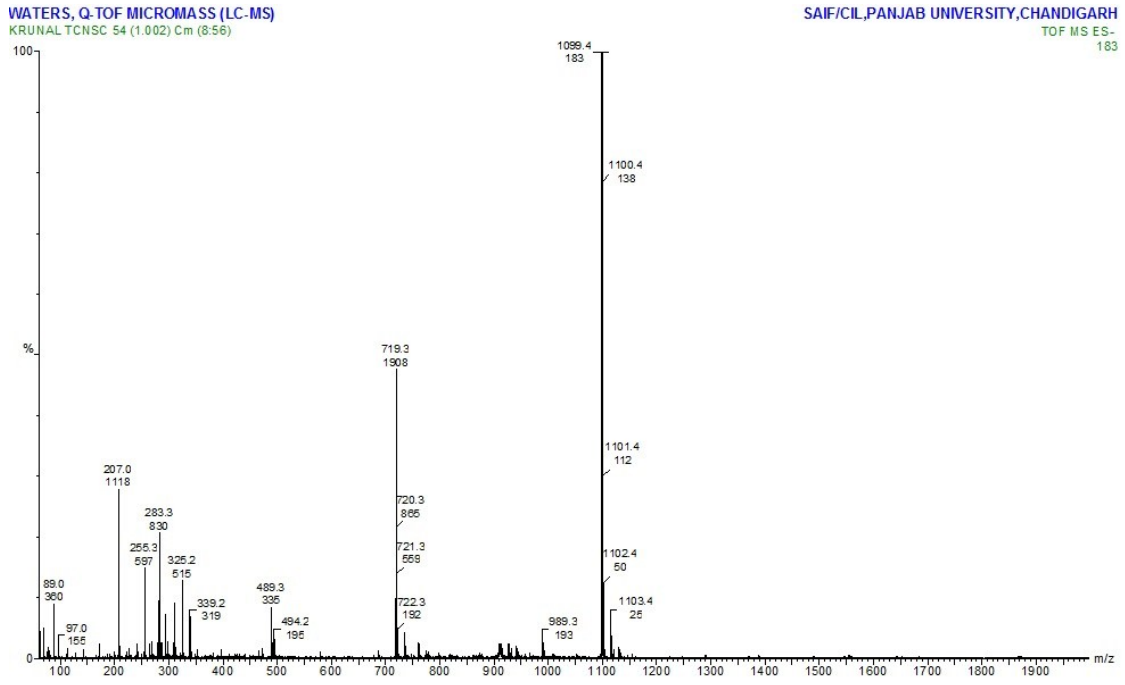

S2 Mass of TCDNS

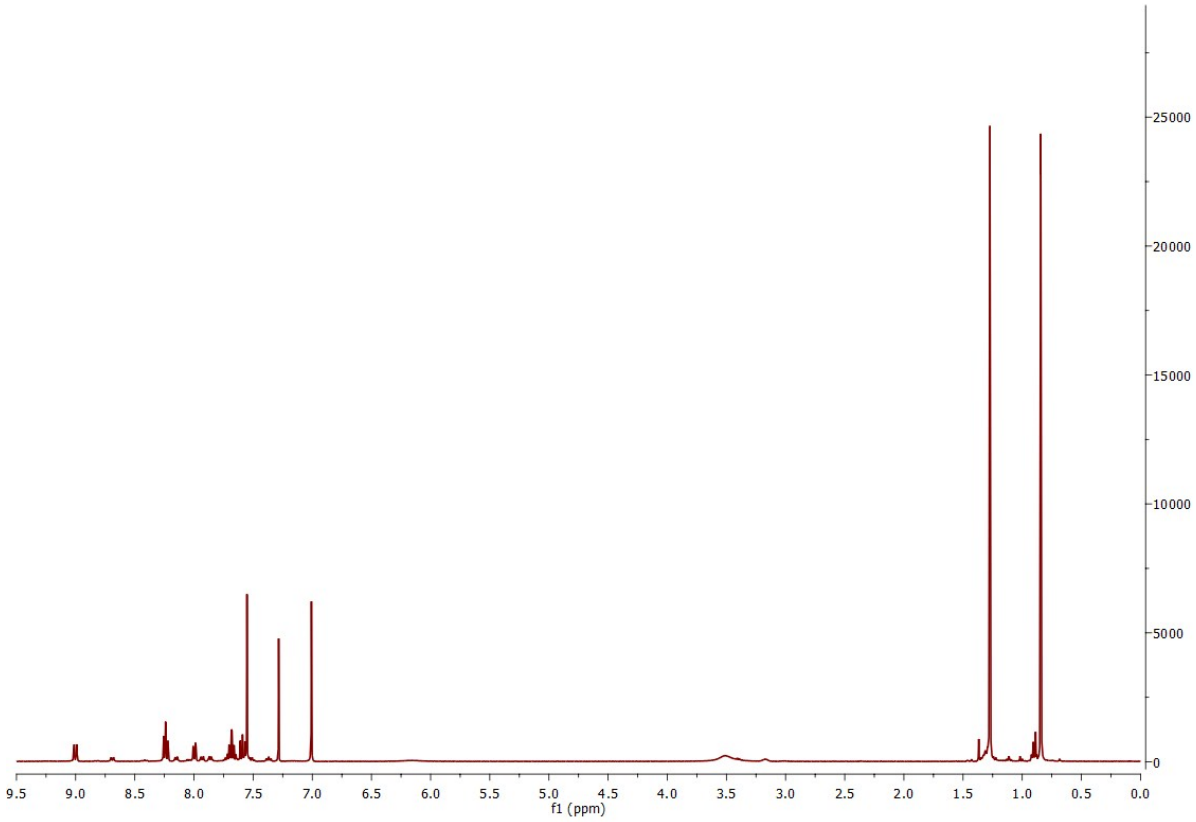

S3 ^{1}H-NMR of TCDNS

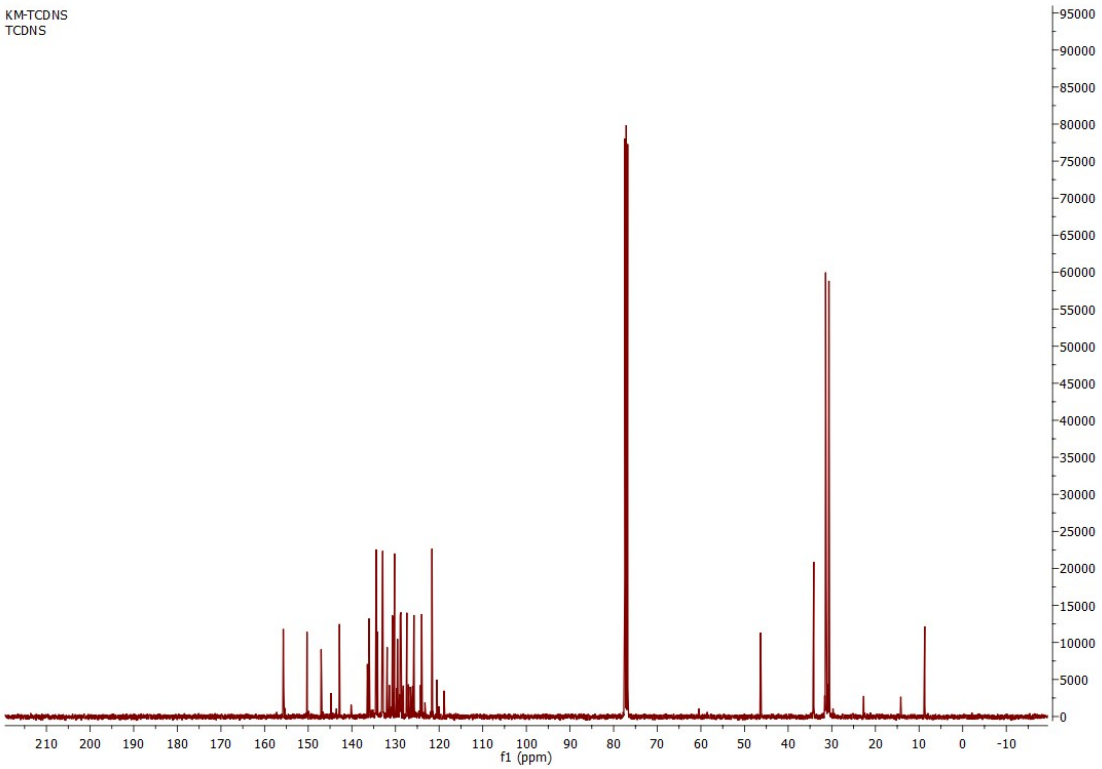

S4 ^{13}C NMR of TCDNS

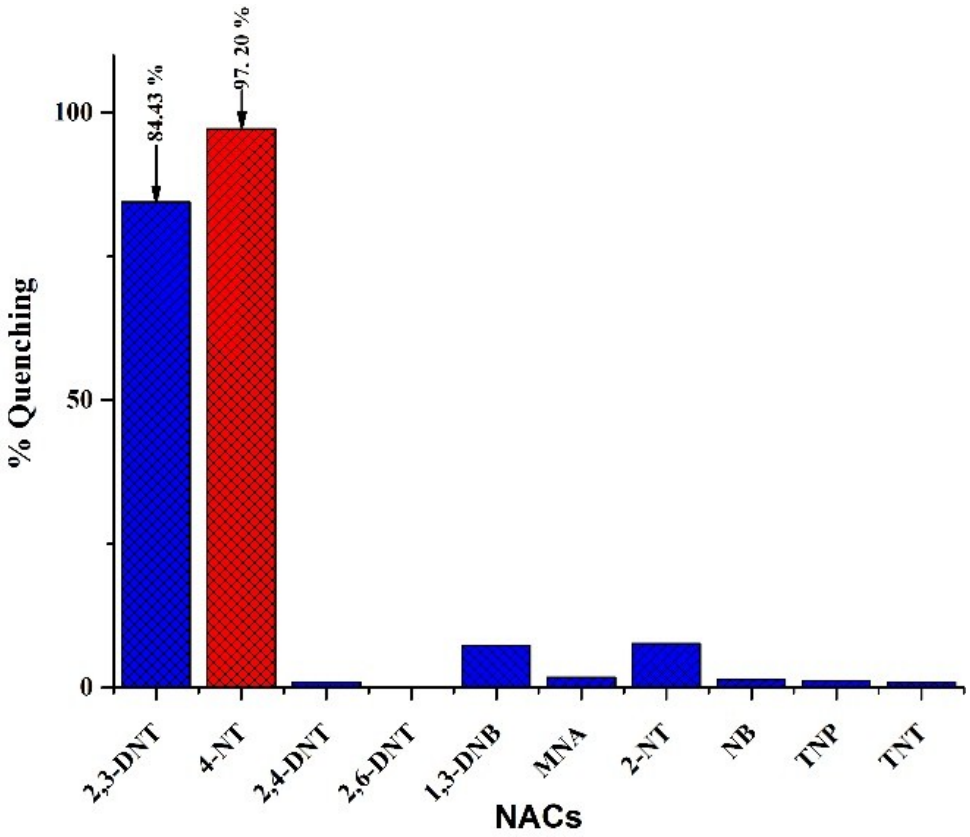

S5 Bar graph showing % quenching of TCDNS upon addition of different NACs

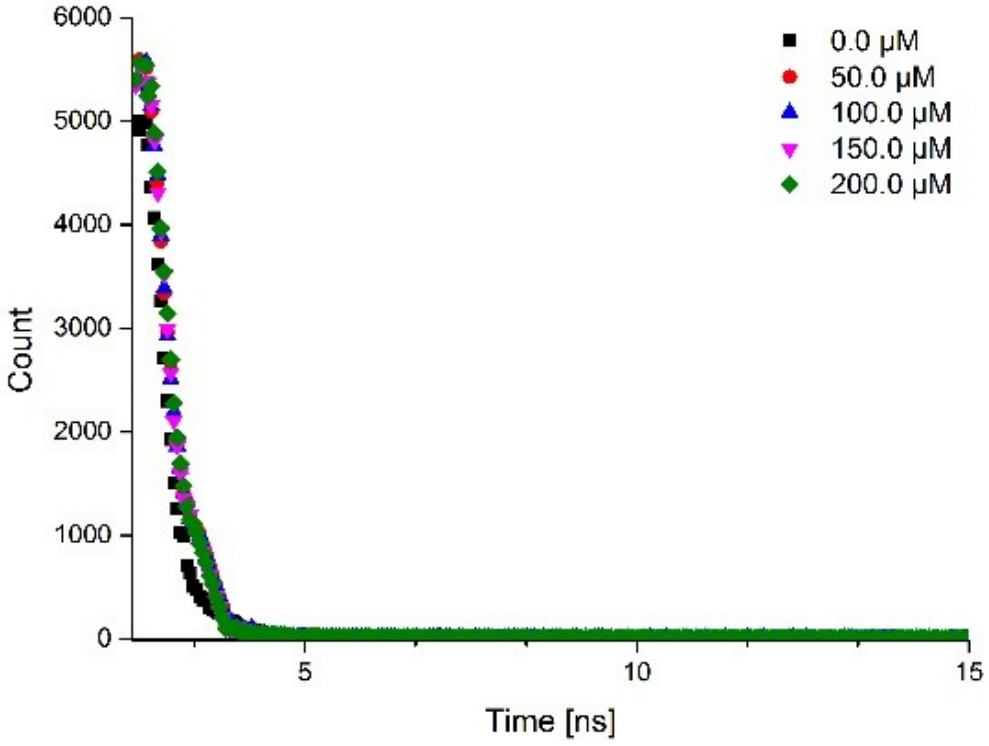

S6 Fluorescence decay curves upon addition of different concentrations (60,120, 180 and 240 µM) of 2,3-DNT. Fluorescence decay curves were monitored at 342 nm

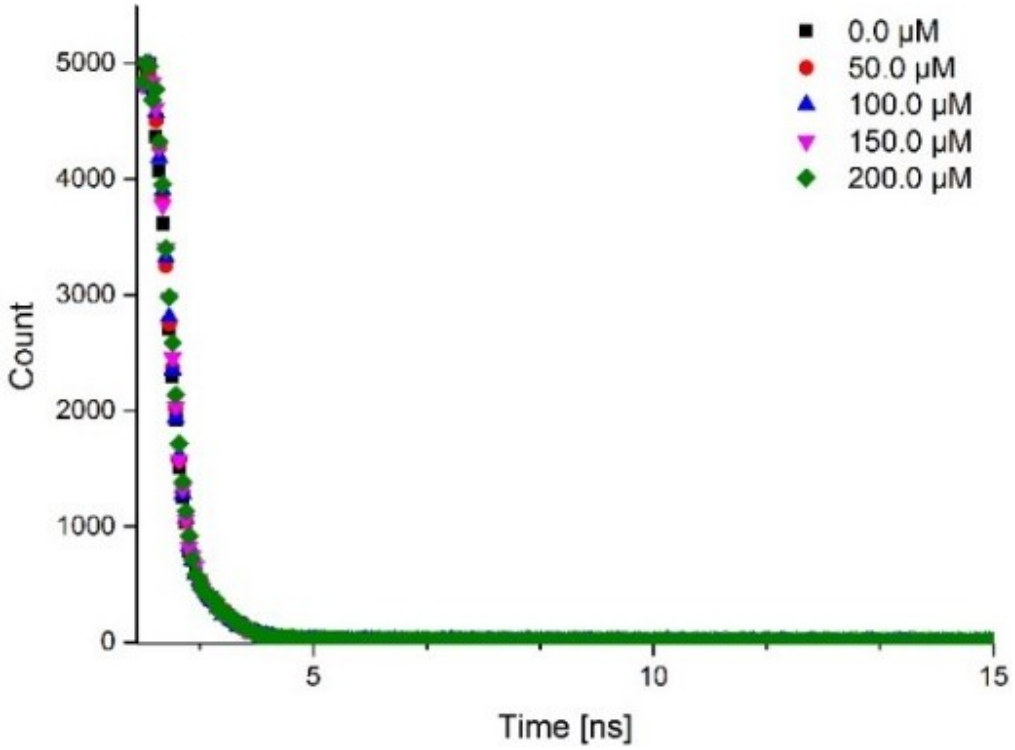

S7 Fluorescence decay curves upon addition of different concentrations (50,100, 150 and 200 µM) of 4-NT. Fluorescence decay curves were monitored at 342 nm

S8 Binding constant and quantum yield for ligand TCDNS in the presence of NACs

Ligand	Selective NACs	Binding Constant (K_s) M^{-1}	Quantum Yield φ	R^2
TCDNS	**2,3-DNT**	**1.66×10^4**	**0.096**	**0.9965**
	4-NT	**2.37×10^5**	**0.015**	**0.9976**

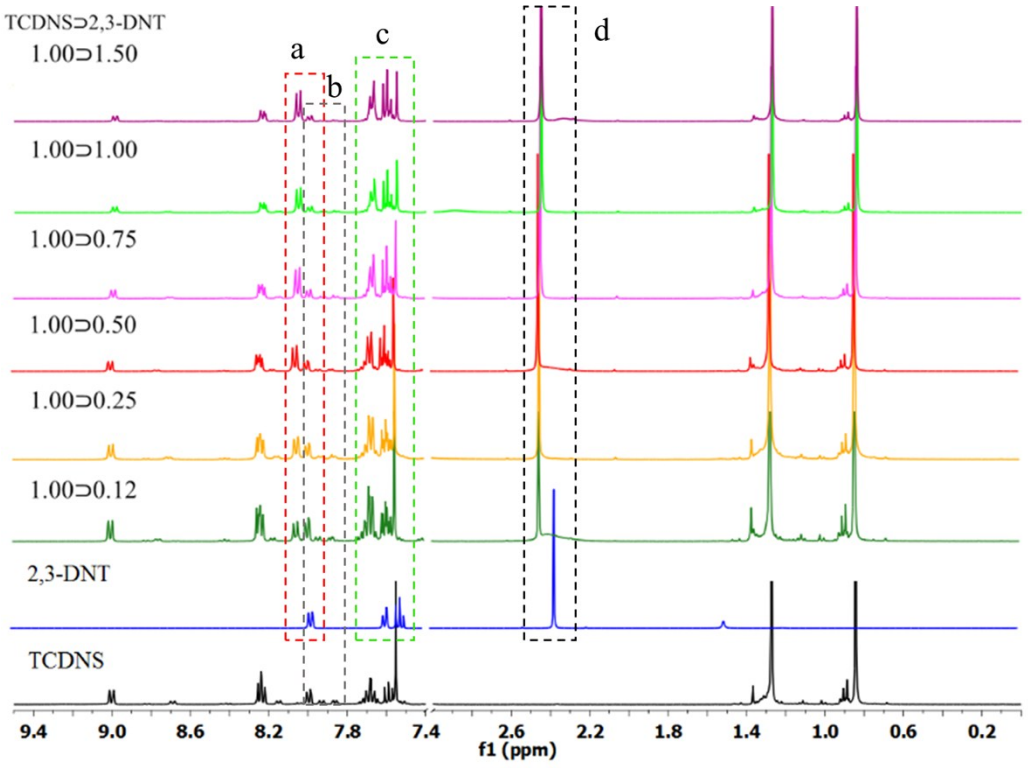

S9 ^{1}H-NMR Titration of TCDNS with (0.12, 0.25, 0.50, 0.75, 1.0, 1.5) equiv. of 2,3-DNT in $CDCl_3$

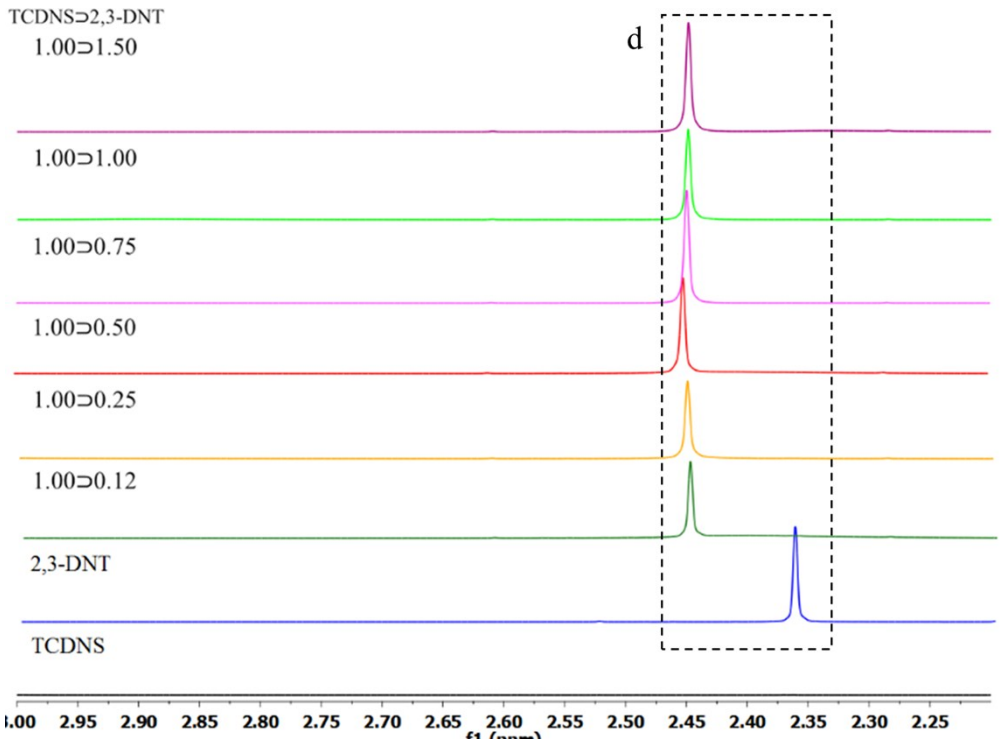

S9 A) Expansion of (d) section in NMR Titration of TCDNS⊃2,3-DNT

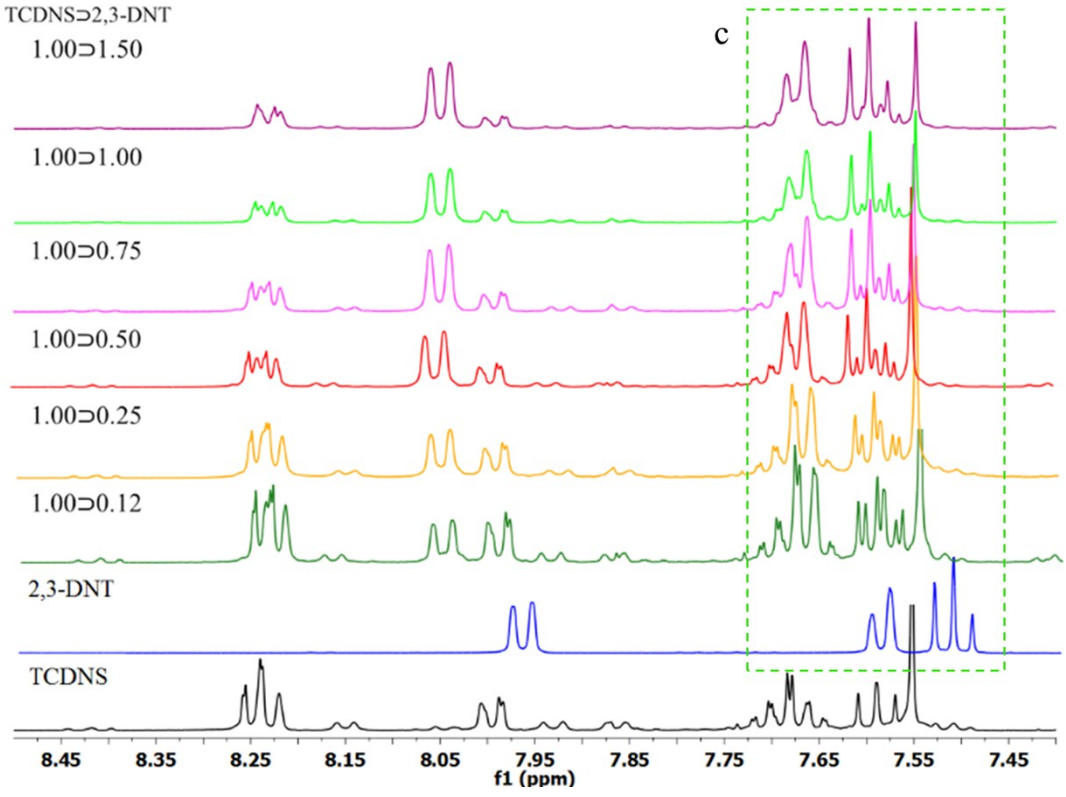

S9 B) Expansion of (c) section in NMR Titration of TCDNS⊃2,3-DNT

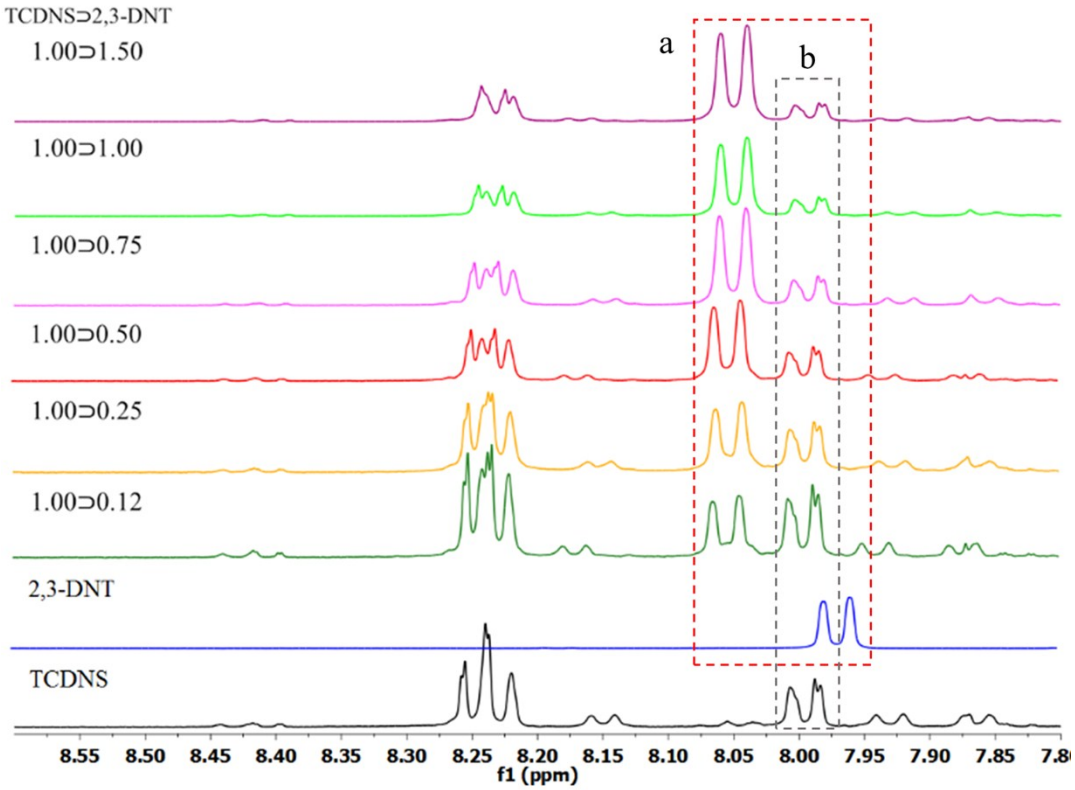

S9 C) Expansion of (a) and (b) section in NMR Titration of TCDNS⊃2,3-DNT

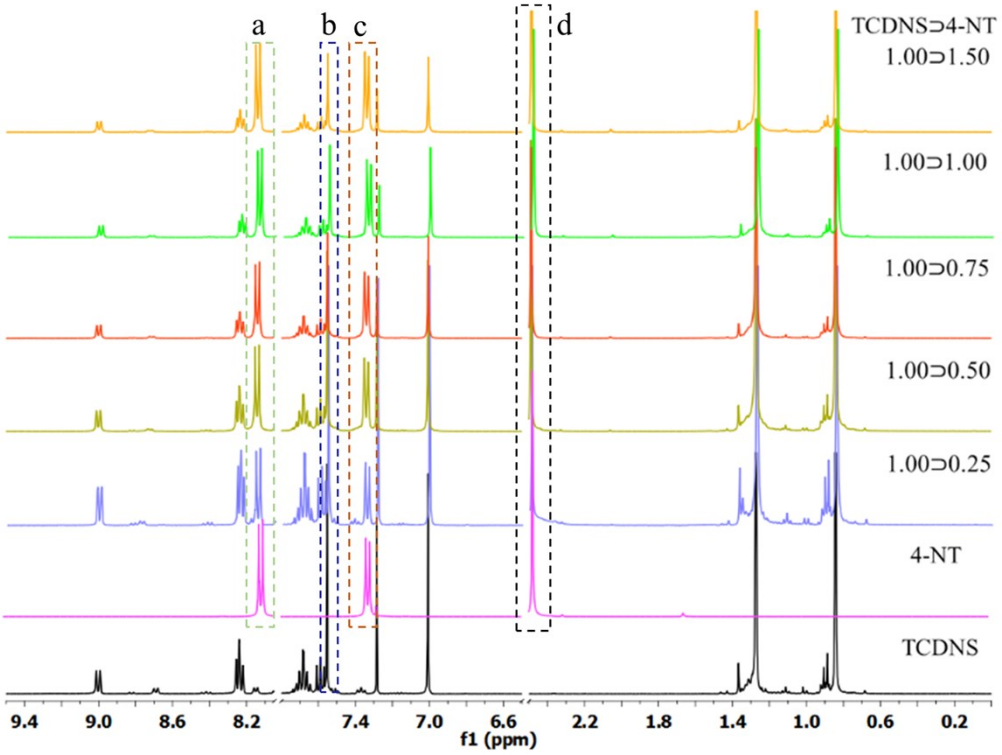

S10 ^{1}H-NMR Titration of TCDNS with (0.12, 0.25, 0.50, 0.75, 1.0, 1.5) equiv. of 2,3-DNT in $CDCl_3$

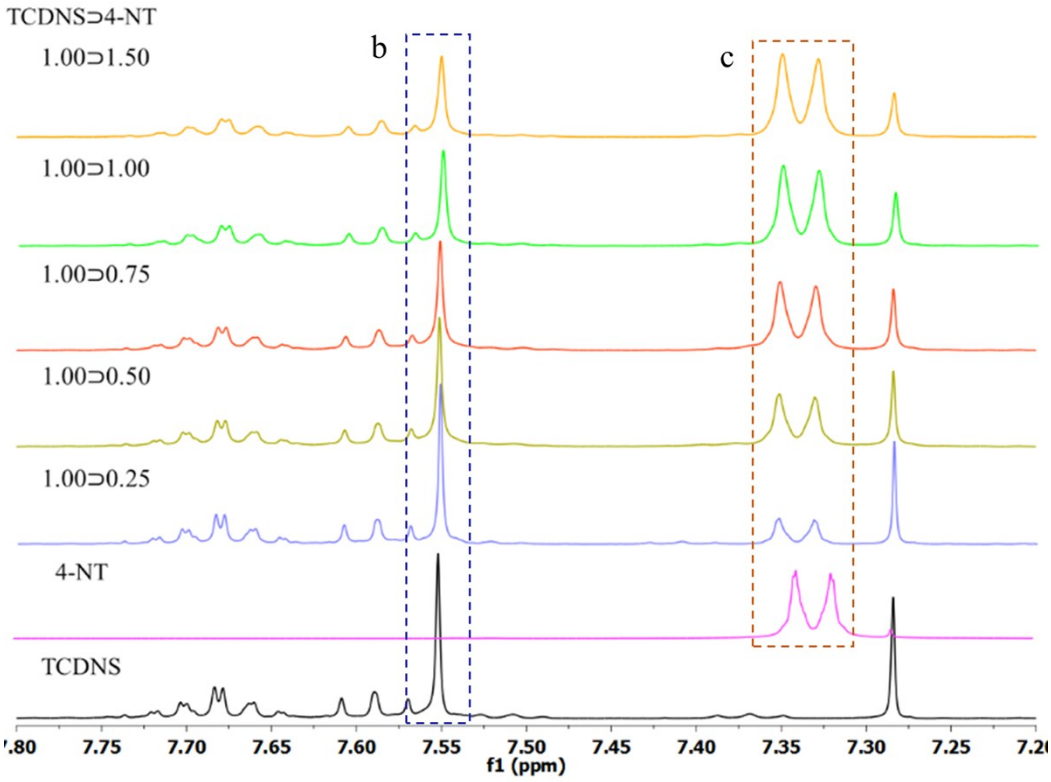

S10 A) Expansion of (b) and (c) section in NMR Titration of TCDNS⊃4-NT

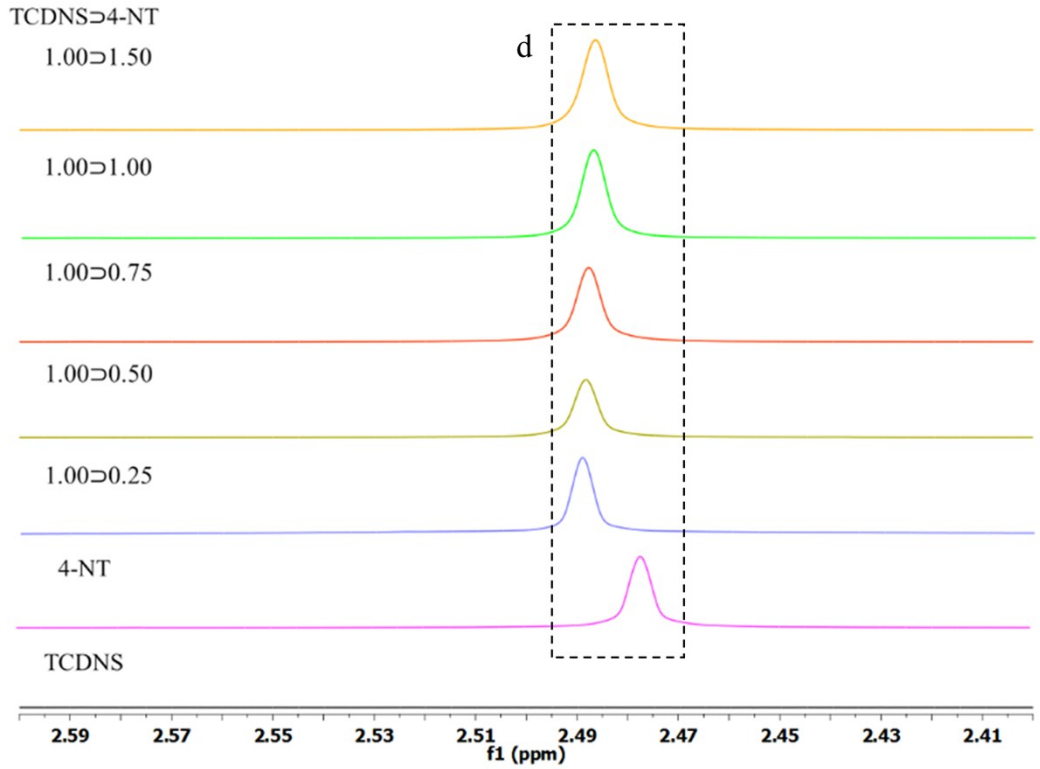

S10 B) Expansion of (d) section in NMR Titration of TCDNS⊃4-NT

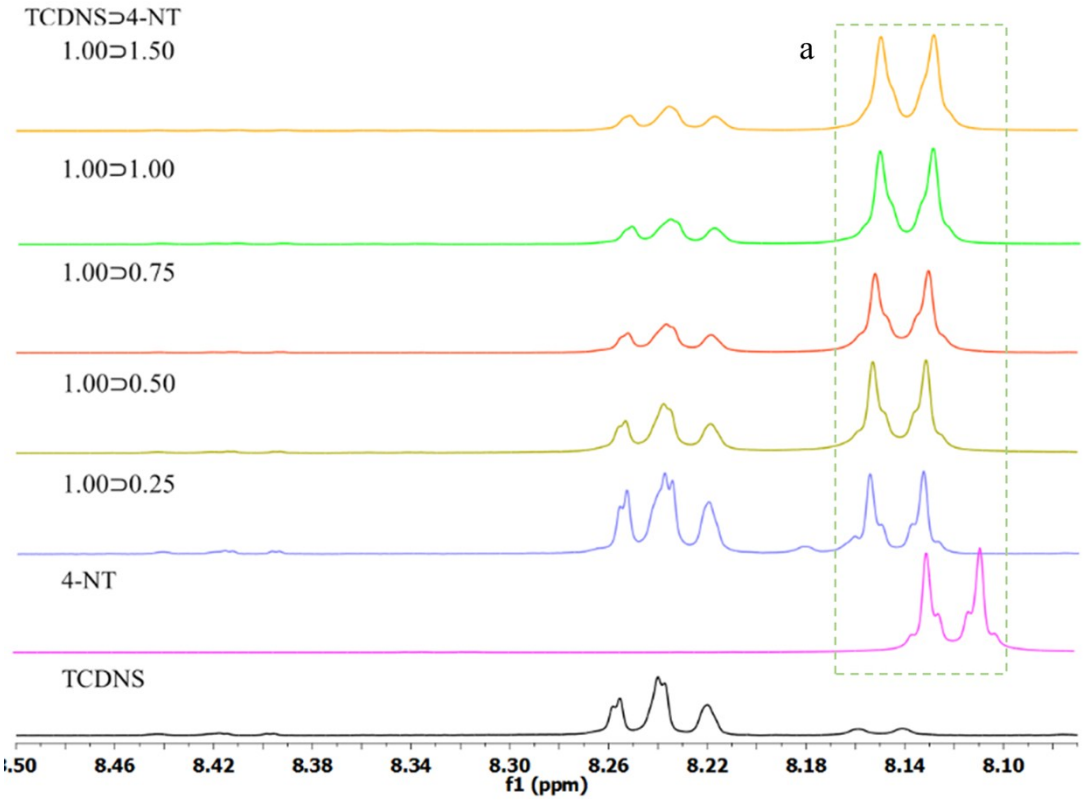

S10 C) Expansion of (a) section in NMR Titration of TCDNS⊃4-NT

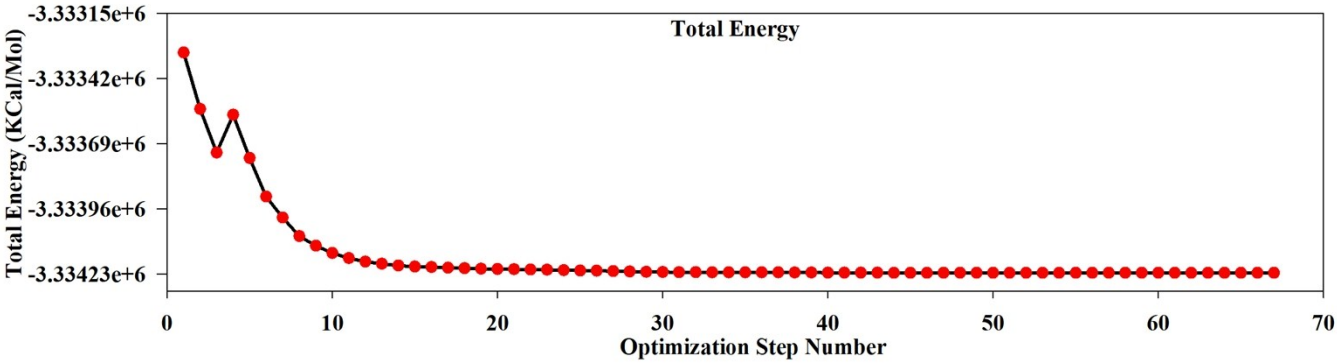

S11 TCDNS geometry optimization total energy graph

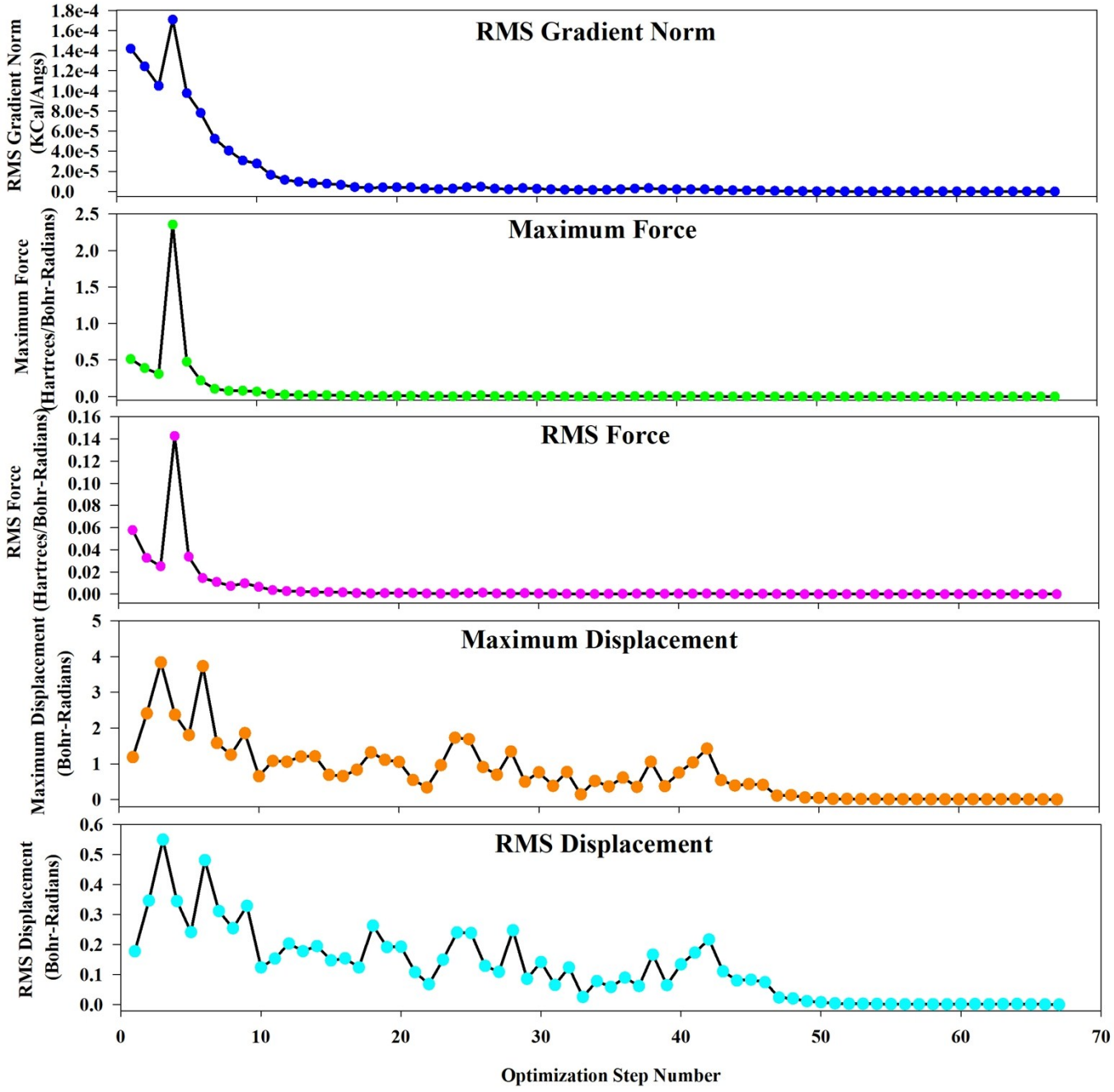

S12 TCDNS geometry optimization other graphs

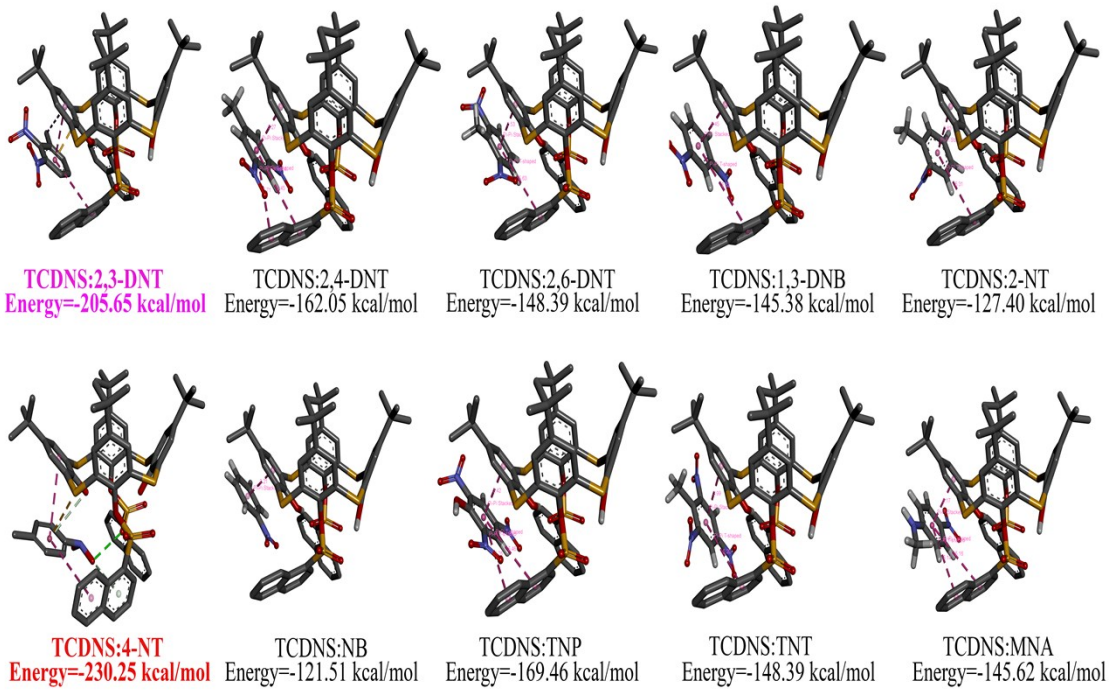

S13 Docking Details of TCDNS with Different NACs

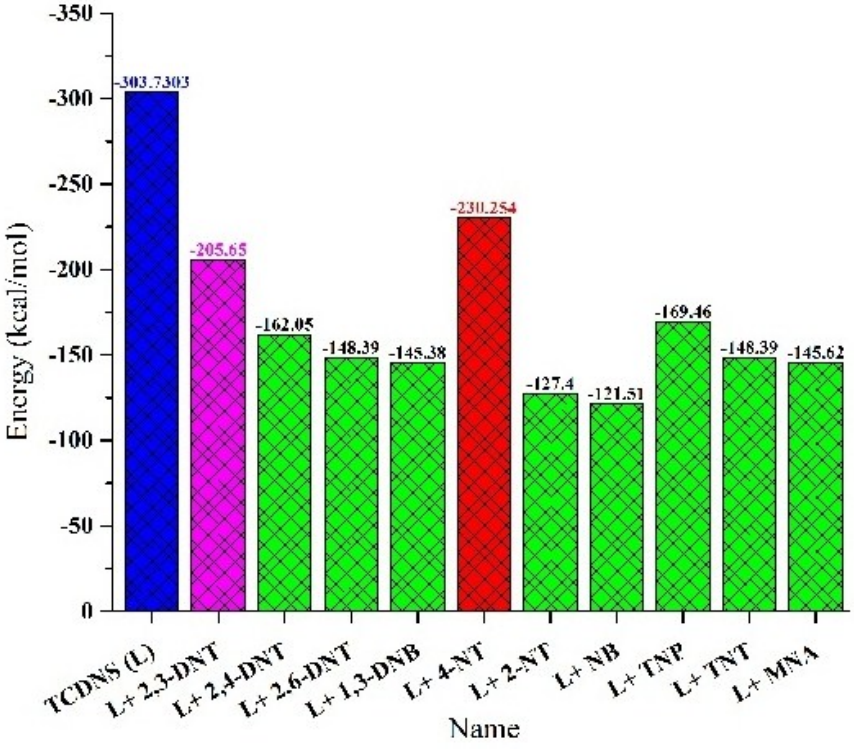

S14 Docking Energy Bar Graph of TCDNS with Different NACs

S15 Molecular docking result

Sr. No	Target	Analyte	Docking energy (kcal/mol)
1	TCDNS	2,3-DNT	-205.65
2		4-NT	-230.25

S16 Statistical (Quality analysis) data for the Molecular dynamics study.

Sr. No.	Parameters	Average		Standard deviation		Slope (ps^{-1})	
		TCDNS⊃2,3-DNT	TCDNS⊃4-NT	TCDNS⊃2,3-DNT	TCDNS⊃4-NT	TCDNS⊃2,3-DNT	TCDNS⊃4-NT
1	Total energy (kcal/mol)	-10713.854	-10713.643	80.951	75.531	0.006	0.005
2	Potential energy (kcal/mol)	-13370.420	-13518.755	22.948	23.961	0.000	-0.000
3	Temperature (K)	298.767	298.751	1.379	1.367	-0.000	0.000
4	Pressure (bar)	-0.415	1.427	92.720	90.417	0.000	-0.000
5	Volume ($Å^3$)	43081.343	43482.319	88.207	90.209	-0.000	-0.000

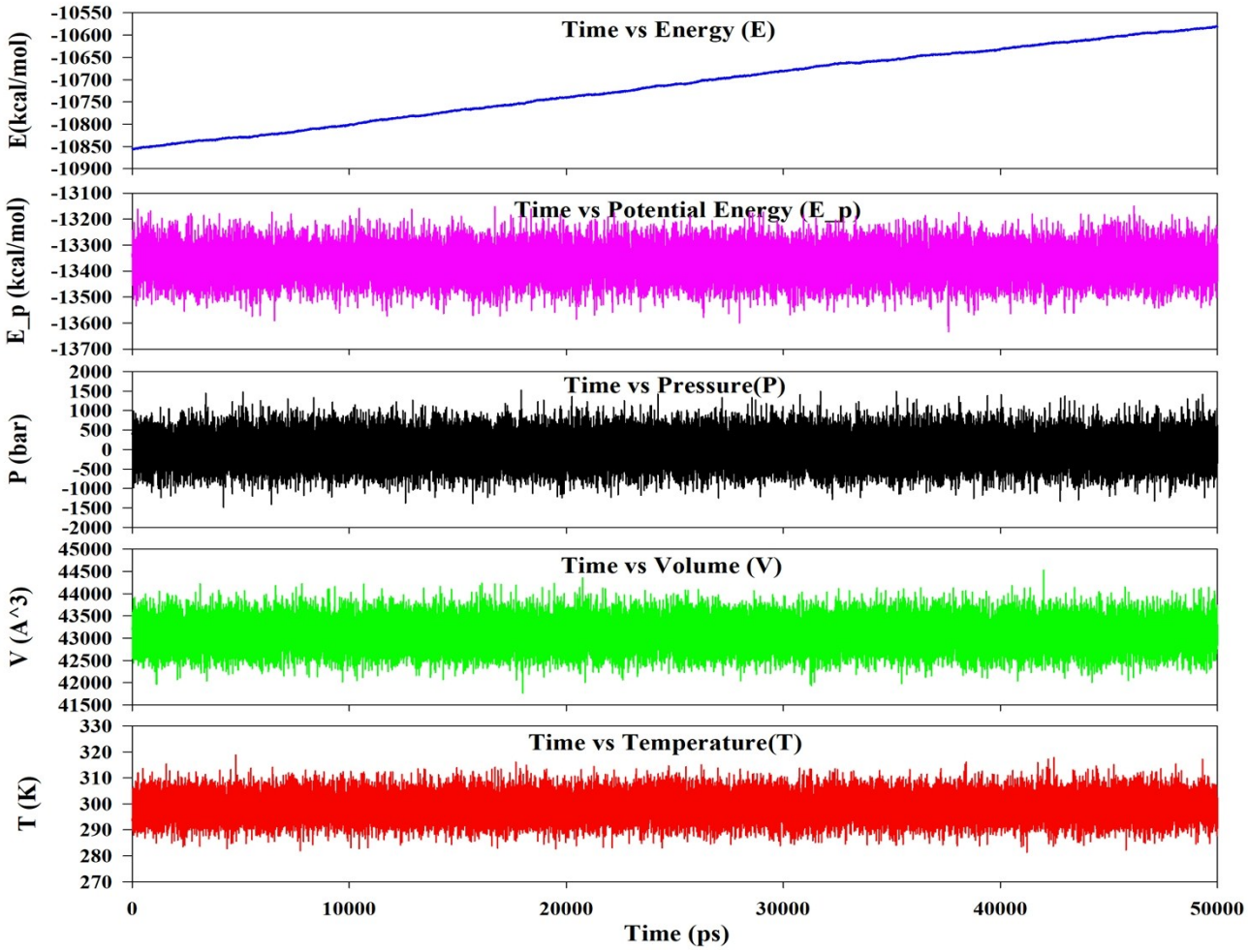

S17 Simulation quality analysis energy graphs of TCDNS⊃2,3-DNT

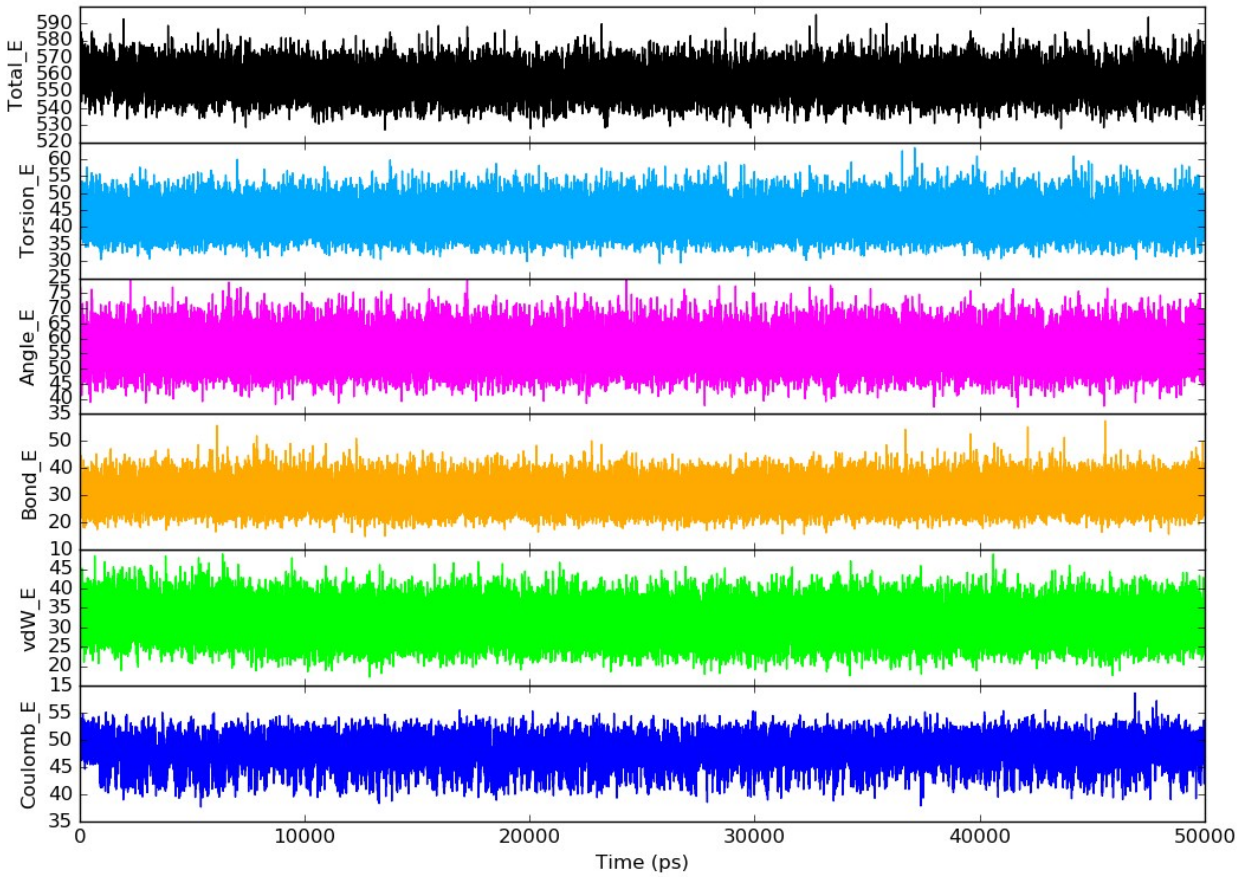

S18 Simulation event analysis energy graphs of TCDNS⊃2,3-DNT.

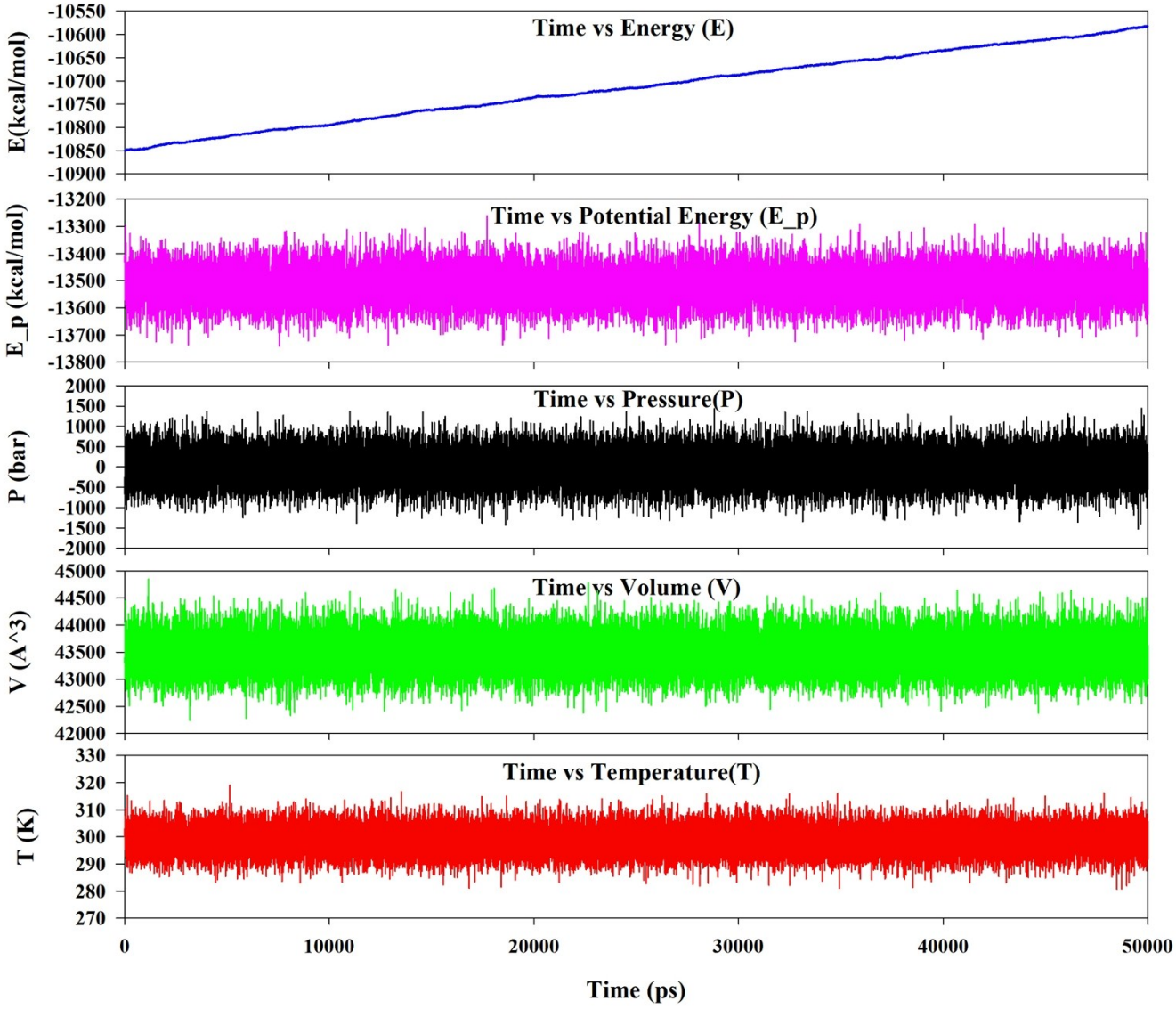

S19 Simulation quality analysis energy graphs of TCDNS⊃4-NT

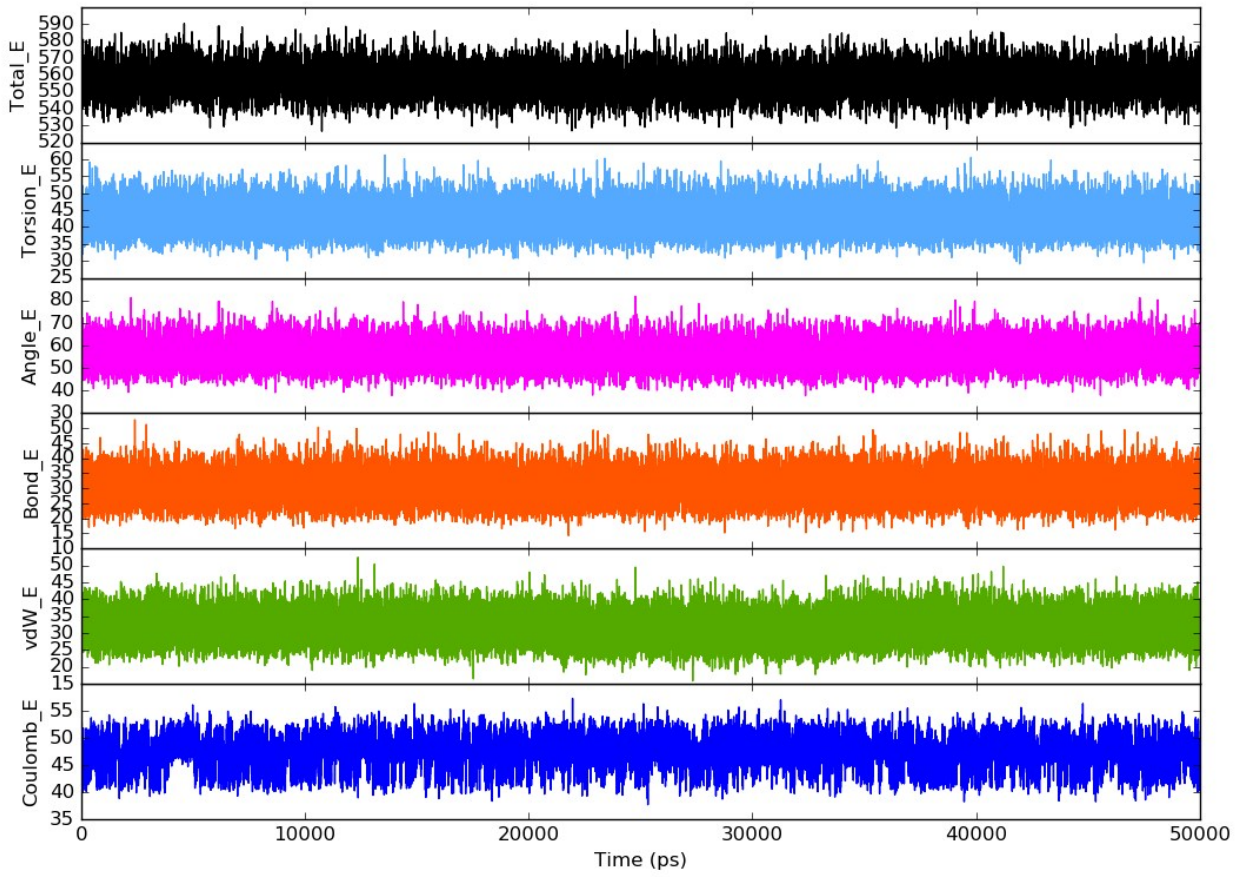

S20 Simulation event analysis energy graphs of TCDNS⊃*4*-NT

S21 LOD calculations for TCDNS with 2,3-DNT and TCDNS with 4-NT[9, 10]

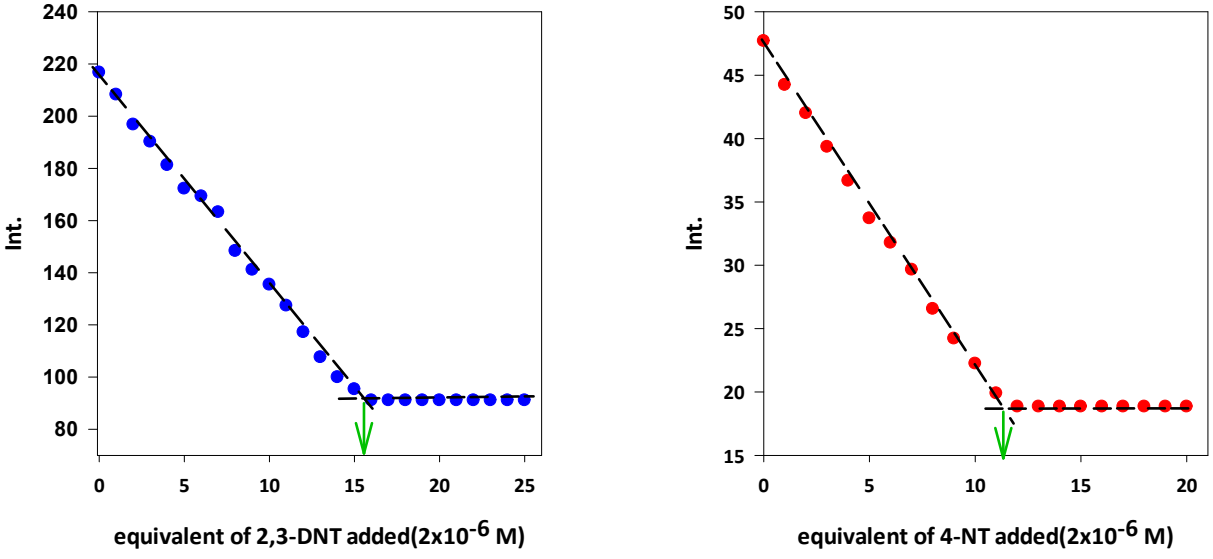

The detection limit was determined by fluorescent titrations. We had added aliquots of 2,3-DNT and 4-NT solution in minimum concentration into the solution of **TCDNS**. Following the addition of

aliquots, a graph of fluorescence intensity as a function of concentration of 2,3-DNT and 4-NT added was plotted, respectively. Then, determination of detection limit was carried out from this graph by multiplying the concentration where there is a sharp change in the fluorescence intensity to the concentration of **TCDNS**.

Equation used for calculating detection limit (DL):

The detection limit was then calculated by using the following equation:

DL = CL × CT

CL = Conc. of Ligand; CT = Conc. of Titrant at which change observed.

Thus;

(A) Detection limit of 2,3-DNT:

$DL = 2 \times 10^{-4} \times 15.50 \times 2 \times 10^{-6} = 6.20 \times 10^{-9}$ M.

(B) Detection limit of 4-NT:

$DL = 1 \times 10^{-4} \times 11.2 \times 2 \times 10^{-6} = 4.48 \times 10^{-9}$ M.

Thus by using the above formula, detection limit (DL) was found to be 6.20×10^{-9} and 4.48×10^{-9} for 2,3-DNT and 4-NT, i.e., **TCDNS** can detect 2,3-DNT and 4-NT in this minimum concentration.

S22 Comparison of various optical methods with those in recent papers on the detection of NACs.

Sr No	Method	% Quenching	Sensing range	Sensor for	Platform	Solvent	Ref
1	Fluorescence technique	92.50	0.72mM	4-NT	Metal-organic framework	DMF	11
2	Fluorescence technique	80.04	-	4-NT	Zn(II)-organic Framework	Water	12
3	Fluorescence technique	27.00	0.50 mM	4-NT	Eu(III)-organic Framework	DMF	13
4	Fluorescence technique	96.52	50.0 µM to 1mM	4-NT	Calix[4]Resorcinarene	5%water:THF	14
5	Fluorescence technique	97.20	4.0 µM to 0.1mM	4-NT	Thiacalix[4]arene	5%water:THF	This work
	Fluorescence technique	84.43	0.5 µM to 0.01mM	2,3-DNT	Thiacalix[4]arene	5%water:THF	

References:

1. J. Blaney, *Journal of computer-aided molecular design*, 2012, **26**, 13-14.
2. S. Mandal, M. n. Moudgil and S. K. Mandal, *European journal of pharmacology*, 2009, **625**, 90-100.
3. M. Frisch, G. Trucks, H. Schlegel, G. Scuseria, M. Robb, J. Cheeseman, G. Scalmani, V. Barone, B. Mennucci and G. Petersson, *See also: URL: http://www. gaussian. com*, 2009.
4. A. W. Kahsai, K. Xiao, S. Rajagopal, S. Ahn, A. K. Shukla, J. Sun, T. G. Oas and R. J. Lefkowitz, *Nature chemical biology*, 2011, **7**, 692-700.
5. J. D. Durrant and J. A. McCammon, *BMC biology*, 2011, **9**, 71.
6. H. Alonso, A. A. Bliznyuk and J. E. Gready, *Medicinal research reviews*, 2006, **26**, 531-568.
7. S. E. Nichols, R. Baron, A. Ivetac and J. A. McCammon, *Journal of chemical information and modeling*, 2011, **51**, 1439-1446.

8. F. R. Salsbury, *Current opinion in pharmacology*, 2010, **10**, 738-744.
9. K. Modi, U. Panchal, V. Mehta, M. Panchal, A. Kongor and V. K. Jain, *Journal of Luminescence*, DOI: http://dx.doi.org/10.1016/j.jlumin.2016.07.019.
10. N. Sharma, S. I. Reja, V. Bhalla and M. Kumar, *Dalton Transactions*, 2015, **44**, 6062-6068.
11. D. Tian, Y. Li, R.-Y. Chen, Z. Chang, G.-Y. Wang and X.-H. Bu, *Journal of Materials Chemistry A*, 2014, **2**, 1465-1470.
12. W.-C. Song, X.-Z. Cui, Z.-Y. Liu, E.-C. Yang and X.-J. Zhao, *Scientific Reports*, 2016, **6**, 34870.
13. X. Zhou, H. Li, H. Xiao, L. Li, Q. Zhao, T. Yang, J. Zuo and W. Huang, *Dalton Transactions*, 2013, **42**, 5718-5723.
14. U. Panchal, K. Modi, S. Dey, U. Prajapati, C. Patel and V. Jain, *Journal of Luminescence*, 2017, **184**, 74-82.